ORIGINAL ARTICLE

Effect of initial conditions on the inhibition process of H_2−O_2/air detonations using CF_3I, CO_2, and H_2O

A. Dahake[1] · R. K. Singh[1] · A. V. Singh[1]

Abstract

The unwarranted leakage/release of hydrogen gas from metal processing, automotive, petrochemical industries, and nuclear reactors, along with its subsequent ignition and transition to detonation, could lead to catastrophic damage to both life and property. The development of practical hazard prevention and safety control systems demands an understanding of the effectiveness of the chemical inhibitors to suppress/mitigate a detonation wave under varying operational conditions. In the current study, the inhibition efficiency of chemical inhibitors under varying mixture initial conditions was investigated using numerical computations. The inhibition efficiency of trifluoroiodomethane (CF_3I), carbon dioxide (CO_2), and steam (H_2O) on hydrogen-oxygen/air mixtures was evaluated using a detailed chemical kinetic model for hydrogen oxidation. ZND computations were carried out over a range of initial mixture composition, pressure, and temperature. It was found that CF_3I is a better inhibitor than CO_2 and H_2O at all the initial mixture conditions. However, at very high temperatures, the inhibitors CF_3I, CO_2, and H_2O have a similar detonation inhibition efficiency. The inhibition efficiency of carbon dioxide and steam is comparable and significantly lower than CF_3I. The findings from the current work can be used to design optimized detonation safety systems over a range of practical operating conditions.

Keywords Inhibitors · Inhibition efficiency · Halons · Detonation inhibition

1 Introduction

Accidental explosions occur during the storage and transportation of fuels, primarily due to gas leaks and fuel spillage. In the case of highly reactive fuels such as hydrogen, the chemical reactions and species molecular diffusion rates are greater than for typical hydrocarbon fuels. Therefore, a flame

✉ A. Dahake
  ashlesh@iitk.ac.in

  R. K. Singh
  ranjay20@iitk.ac.in

  A. V. Singh
  ajayvs@iitk.ac.in

[1] Department of Aerospace Engineering, Indian Institute of Technology Kanpur, Kanpur, Uttar Pradesh 208016, India

accelerates rapidly, leading to fast deflagrations or even a detonation through the deflagration-to-detonation transition (DDT) phenomenon. It is well known that gaseous detonations resulting from the formation of an explosive mixture due to the uncontrolled release of flammable gas and an oxidizer are the most destructive accident scenarios. A fully developed detonation wave propagates at supersonic velocities (> 1800 m/s), reaching overpressures of more than 20 bars. The mechanical load associated with a shock wave of such high overpressures is a major destructive factor. Therefore, Wang et al. suggested that the flame acceleration and the DDT phenomenon must be taken into consideration for safety and hazard evaluation [1].

Hydrogen is a very reactive clean fuel and is believed to be a future energy carrier. Hydrogen is seen as a universal remedy to address problems related to global warming, increased air pollution, and fossil fuel depletion. However, the primary concern for adopting hydrogen as a suitable alternative to the currently used energetic fuels is the safety aspects associated with possible gas leaks and hydrogen hazards. Due to the low ignition energy and wide explosion limit of hydrogen, several hydrogen explosion accidents have been reported in

the production, storage, and refueling stations [2]. Hydrogen being a small molecule, and due to its low viscosity, is more prone to leakages from pipeline connections as compared to larger hydrocarbons. It was found that hydrogen leaks three times and five times faster than natural gas and propane, respectively, on a volumetric basis [3]. The leakage of hydrogen from storage tanks or transport pipelines results in the formation of a large vapor cloud; the hydrogen vapor mixes with air and forms a flammable mixture before ignition occurs. Vapor cloud explosions have been widely studied in the literature due to their resemblance to practical explosion scenarios [4–9]. Oran et al. showed that such vapor clouds under favorable conditions could undergo DDT even in the absence of any confinement and could lead to loss of life and resources [7, 8]. Jiang et al. carried out experimental studies on unconfined hydrogen explosions in the presence of external turbulence. It was found that the cumulative effect of external turbulence and the inherent flame instabilities could result in flame acceleration [9]. Also, the blast wave overpressures for a partially confined detonation were found to be significantly greater than an unconfined detonation for the same amount of fuel [10]. In the case of nuclear reactors, hydrogen gas can be formed by the reaction of zirconium and steam at elevated temperatures during a severe accident. Also, hydrogen can be formed in light water-cooled reactors due to the radiolytic decomposition of water [11]. The damage reported at the Fukushima nuclear plant (2011) resulted from an intense hydrogen explosion [11]. Thus, there is a great interest in hydrogen flammability and detonability limits and their implications for safety and prevention in many applications.

The use of chemical inhibitors and diluents for detonation and fire suppression has been widely studied by researchers worldwide [12–22]. The chemical inhibitors, when added to a fuel-oxidizer mixture, interfere with the oxidation chemistry. The primary objective of the addition of a chemical inhibitor to a fuel-oxidizer mixture is to alter the mixture's detonability and thus reduce detonation hazard. Halogenated hydrocarbons, especially those containing more than one halogen compound, have been found to be very effective in detonation inhibition [12]. Brominated additives such as bromotrifluoromethane or Halon 1301 (CF_3Br) and bromochlorodifluoromethane or Halon 1211 (CF_2BrCl) have been found to be excellent additives for fire suppression in a given fuel-air mixture [13]. However, their production and use in fire suppression have been banned by the Montreal Protocol because of the high ozone depletion potential of bromine [14, 15]. The bromine atoms from the brominated compounds reach the stratosphere and are a major ozone depletor. In the recent past, efforts were devoted to find a suitable replacement for Halon 1301 with similar suppression ability and also environment-friendly production and application. It was found that iodinated hydrocarbon could

be a suitable replacement. Leclerc et al. [14] conducted an experimental study on methane oxidation in the presence of trifluoroiodomethane (CF_3I) to evaluate the inhibiting effect. It was found that CF_3I is as good an inhibitor as brominated compounds [14]. The addition of chemical inhibitors reduces the rate of bimolecular reactions. The addition of CF_3I to hydrocarbon fuels such as methane, propane, and acetylene was observed to reduce the laminar flame speed by consuming the active radicals and producing fewer reactive radicals [15]. Moen et al. evaluated the detonation inhibition efficiency of various inhibitors [16]. The experimental results showed that CO_2 as a diluent has a better detonation inhibition tendency than CF_3Br for fuel-air and fuel-oxygen mixtures. It was found that dilution with nitrogen and carbon dioxide leads to a change in the thermodynamic properties of a fuel-oxidizer mixture. The addition of these diluents reduces the thermal diffusivity and thermal conductivity of the fuel-oxidizer mixture, thereby reducing the flame speed of the mixture [17]. Kumar and Singh performed numerical computations to study the efficacy of CF_3I, H_2O, CO_2, and N_2 for suppressing H_2–O_2/air detonations. The results suggested that H_2O is a better inhibiting agent than CF_3I based on the retardant weight required to suppress a detonation wave [14]. It was also found that CF_3I has a detonation promotion effect at lower concentrations (< 6000 PPM), and the expected inhibition effect is observed at higher additive concentrations for H_2–O_2 mixtures. The promotion effect of CF_3I at lower concentrations is due to an increase in the production of H radical through $I + H_2 \rightarrow HI + H$, whereas at higher concentrations, the reaction, $H + CF_3I \rightarrow HI + CF_3$ dominates and consumes the reactive H radical leading to detonation inhibition [18]. Thus, the inhibition effect of CF_3I, a potential Halon 1301 (CF_3Br) replacement, is well documented in the literature. However, the studies reported in the literature are specifically carried out at stoichiometric conditions and standard initial pressure and temperature. The hydrogen explosions occurring, especially in confined spaces and nuclear reactors, can have a range of initial mixture composition and pressure-temperature variations. The boiling water reactors and pressurized water reactors operate at very high initial pressures; also, partially combusted fuel-oxidizer mixtures can heat the unburned mixture and change the initial thermodynamic state of the flammable mixture [11]. Therefore, it is important to study these chemical and thermal inhibitors over a range of mixture initial conditions. However, the literature regarding this is minimal [23]. As such, no literature is available to the author's knowledge in which a systematic study of the effect of a mixture's initial thermodynamic state on the inhibition efficiency of halogenated inhibitors has been carried out. Therefore, in the present work, we attempted to evaluate the effect of varying initial conditions on the inhibition efficacy of detonation inhibitors.

Gaseous detonations are characterized by a cellular structure resulting from strong interactions between the incident shock, the transverse waves, and Mach stems [24]. The detonation cell size is quantified based on the average width of the detonation cell, which is the spacing between transverse waves of the same family. The detonation cell width (λ) depends on the type of fuel and oxidizer, the fuel-oxidizer stoichiometry, the initial thermodynamic state of the reactive mixture, dilution, etc. The detonation cell width is the most prominent detonation parameter and has been extensively studied due to its relation to different detonation propagation parameters [25–28]. Researchers in the past have used simplified one-dimensional analysis (i.e., ZND detonation model) to predict the dynamic detonation parameters. It was found that the ZND reaction length (Δ) correlates linearly with the cell width of multi-dimensional detonations [29–32], i.e., $\lambda = A\Delta$. The value of A changes by more than an order of magnitude for different fuel-oxidizer-diluent mixtures [29, 30]. Further efforts were devoted at refining the correlation by developing elaborative theoretical approaches for the ratio of the cell width to the induction length. Gavrikov et al. proposed an approach to generalize the correlation ($\lambda = A \times \Delta_i$) by considering the multi-dimensional structure of detonations. The proportionality constant A was considered to be a function of two stability parameters [dimensionless effective activation energy (ε_I) and a parameter describing the relation between chemical energy and the initial thermal energy of the combustible mixture (T_{vN}/T_0)] [29]. Ng et al. also developed a correlation where A was defined as a function of the non-dimensional stability parameter ($\chi = \varepsilon_I \times \Delta_i \frac{\dot{\sigma}_{max}}{u_{CJ}}$) with empirically fitted coefficients [33]. Mevel et al. proposed a correlation with $A = 30\Phi^{-0.233}\left(1 - X_{N_2}\right)^{0.098}(P_1/P_0)^{0.699}$ as a function of mixture equivalence ratio, nitrogen mole fraction (X_{N_2}), and the ratio of initial to standard pressure (P_1/P_0); it predicted the cell width with a mean relative error of 28% for H_2–N_2O (-N_2) mixtures [34]. Zhang et al. proposed a correlation with A having a similar functional form as given by Mevel et al. and including the effect of argon dilution for H_2–N_2O-Ar mixtures, i.e., $A = 25.68\Phi^{-0.112}\left(1 - X_{Ar}\right)^{-1.23}(P_1/P_0)^{0.016}$ [35]. The primary difference between the two expressions of A is the exponent of the diluent term $(1 - X_{dil})$. The induction length does not change much with argon dilution due to the two competing effects: an increase in the specific heat ratio (γ) and a decrease in the total energy release [35]. However, experimental observation reveals increased cell width with increasing argon dilution. Therefore, to keep A increasing progressively, the exponent of the diluent term (argon molar fraction) was thus set to be negative [35].

Although the one-dimensional detonation model does not incorporate the entire structure of the multi-dimensional detonation, it has been historically used to predict the detonation cell width using the induction length based on detailed chemical kinetics. The use of such a simplified model can significantly reduce the computational costs and time. It allows the study of fuel oxidation chemistry over a range of initial conditions and fuel-oxidizer combinations using detailed kinetic reaction mechanisms. The addition of chemically active inhibitors increases the induction length of a ZND detonation, which indicates a loose coupling between the reaction zone and the leading shock wave and thus qualitatively represents less detonable mixtures. Thus, chemical inhibitors are critical in reducing the detonability hazards of practical fuels, and their effectiveness under varying initial conditions warrants further study.

The efficiency of detonation inhibitors can be evaluated based on various detonation parameters such as the detonation cell width, ZND induction zone length, CJ detonation velocity, and the weight of the inhibitor required [18]. Along with the detonation parameters, the economic feasibility of a particular inhibitor can also be used as a limiting parameter for ranking the effectiveness of a given inhibitor over a range of mixture conditions. However, the use of the cell width or the ZND induction zone length based on detailed chemical kinetics has been proven to be the most appropriate parameter to evaluate the efficiency of various inhibitors [12]. Therefore, in the present study, the factor by which a given inhibitor increases the induction zone length of H_2–O_2/air detonations is used as an indicative parameter of the inhibition efficiency.

In the present study, the effect of the initial thermodynamic state of the fuel-oxidizer mixture on the inhibition efficiency of CF_3I, CO_2, and H_2O was evaluated. The primary objective of the present work is to study the influence of initial mixture conditions on the efficiency of detonation inhibitors using a detailed chemical kinetics model for hydrogen oxidation. The computations include varying the initial mixture composition, initial pressure, and temperature of H_2–O_2/air–CF_3I/CO_2/H_2O mixtures.

2 Methodology

In the present work, the one-dimensional ZND detonation model was used to study the efficacy of detonation inhibitors on H_2–O_2/air mixtures at different initial conditions. The modified version of the Caltech Shock and Detonation Toolbox was used for the ZND computations [36]. The chemical kinetic computations were carried out using CANTERA [37] integrated with MATLAB. The Foundational Fuel Chemistry Model – 1(FFCM-1) was used to model hydrogen oxidation. The FFCM-1 model consists of 39 species and 301 reactions [38]. The mechanism adopted by Leclerc et al. for CF_3I was incorporated into the FFCM-1 reaction mechanism to
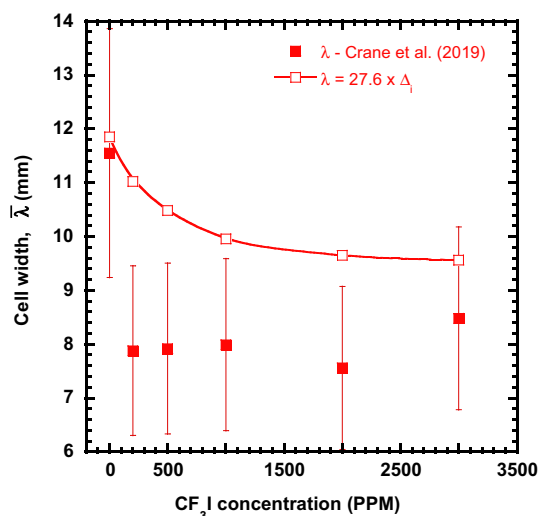
Fig. 1 Effect of varying CF₃I concentration on the detonation cell width. The filled symbols represent the experimental cell width data from Crane et al. [32], and the hollow symbols represent the predicted cell width based on the induction length correlation ($\lambda = 27.6 \times \Delta_i$) given in [32]. The induction length was evaluated under similar conditions using the combined FFCM1-CF₃I model

model CF₃I chemistry [14]. In our previous work [18, 39], it was highlighted that other models describing CF₃I chemistry (Mathieu et al. [15] and Babushok et al. [21]) were not able to capture the ignition promotion effect shown by CF₃I at lower concentrations. However, the CF₃I sub-mechanism from Leclerc et al. [14] was able to predict the ignition promotion effect of CF₃I at low concentrations and produced results that were in excellent agreement with previous experimental results for hydrogen-oxygen detonations [32]. The comparison between the predicted cell width and the experimentally measured cell width is shown in Fig. 1.

The reaction zone in a standard ZND detonation model includes the induction zone and the recombination zone. The induction zone is dominated by two-body chain branching and radical generation reactions, whereas the recombination zone is dominated by three-body chain-terminating reactions. The induction zone length is a characteristic detonation length scale of the standard one-dimensional ZND model. It is now known that a smaller induction length is indicative of more reactive mixtures. A larger induction zone length denotes a slower reaction, and if the induction length is large enough, the reaction zone can be completely decoupled from the leading shock front. However, the shock and reaction front can propagate independently if a sufficient flammable mixture is available [18]. It must also be noted that the leading shock and the reaction zone can again become coupled and propagate as a detonation wave under favorable conditions. Thus, the increase in the induction length indicates a corresponding decrease in the detonability of a given fuel-oxidizer

mixture. Therefore, in order to rank the inhibitor efficiency, the induction length is utilized as a governing parameter.

The inhibition efficiency of an inhibitor is given by the factor of increase (f) in the induction length/time with the addition of inhibitor at the same concentration levels for all the inhibitors. A higher factor of increase in the induction length or time indicates higher efficiency of a detonation inhibitor and vice versa. The factor of increase in the induction length (f_Δ) is the ratio of induction length with inhibitor to without inhibitor for H₂–O₂/air-inhibitor detonations. It is given by

$$f_\Delta = \frac{\Delta_{i, \text{ inhibitor}}}{\Delta_{i, \text{ no inhibitor}}}$$

Similarly, the factor of increase in the induction time (f_τ) is given by

$$f_\tau = \frac{\tau_{i, \text{ inhibitor}}}{\tau_{i, \text{ no inhibitor}}}$$

Kumar and Singh, in their work, pointed out the dual nature of CF₃I addition to H₂–O₂/air mixtures. They observed detonation promotion at a small molar concentration of CF₃I addition (<1200 PPM for H₂–air mixtures and <6000 PPM for H₂–O₂ mixtures) [18]. Therefore, in order to overcome the ambiguity of any promotion effect, the concentration of the inhibitor addition was fixed as 50,000 PPM or 5% molar concentration. The ZND computations were carried out at these concentration levels, and no promotion effect was observed. Therefore, the inhibitor concentration of 50,000 PPM or 5% molar concentration was used for further computations.

3 Results and discussion

3.1 Effect of varying equivalence ratio on the inhibition efficiency

3.1.1 H₂–O₂/air–CF₃I mixtures

The induction length/time and the corresponding factor of increase were evaluated for H₂–O₂/air–CF₃I mixtures with 5% CF₃I addition at an initial pressure of $P_0 = 1$ bar, and initial temperature of $T_0 = 295$ K (refer to Table 1 and Figs. 2 and 3). It is known that CF₃I shows a chemical inhibition effect at higher concentrations, where it drastically increases the induction length/time [18]. The chemical inhibition effect of CF₃I is primarily due to the radical scavenging of active radicals (specifically H radical) in the combustion environment. The recombination of active radicals with the halogenated atom is the major inhibition step for all halogenated inhibitors. The reaction cycle responsible for the

Table 1 Critical detonation parameters (T_{vN}, Δ_i, and τ_i) and the factor of increase (f_Δ, f_τ) at various mixture equivalence ratios (Φ) with and without inhibitors for H_2–O_2/air mixtures

	Φ	H_2–O_2					H_2–air				
		T_{vN} (K)	Δ_i (mm)	τ_i (µs)	f_Δ	f_τ	T_{vN} (K)	Δ_i (mm)	τ_i (µs)	f_Δ	f_τ
No inhibitor	0.4	1621.6	0.054	0.134	–	–	1155.3	69.21	224.8	–	–
	1.0	1761.6	0.050	0.096	–	–	1535.4	0.215	0.573	–	–
	2.0	1724.9	0.102	0.157	–	–	1470.1	0.387	0.924	–	–
5% CF₃I	0.4	1459.1	2.863	9.67	53.1	72.1	934.5	ND*	ND*	ND*	ND*
	1.0	1605.8	0.764	2.18	15.2	22.8	1326.3	50.15	166.9	233.2	290.8
	2.0	1545.5	2.072	5.28	20.4	33.5	1285.5	69.14	210.9	178.6	228.2
5% CO₂	0.4	1545.4	0.077	0.21	1.44	1.54	1080.5	290.2	985.3	4.2	4.38
	1.0	1674.8	0.066	0.14	1.31	1.44	1438.1	0.395	1.13	1.8	1.97
	2.0	1633.6	0.132	0.24	1.32	1.50	1363.2	0.935	2.54	2.4	2.75
5% H₂O	0.4	1577.2	0.080	0.20	1.49	1.52	1107.1	274.8	897.5	3.9	3.99
	1.0	1712.3	0.065	0.13	1.299	1.34	1480.4	0.390	1.06	1.8	1.84
	2.0	1669.1	0.134	0.22	1.316	1.39	1407.1	0.960	2.36	2.5	2.56

*ND – No detonation
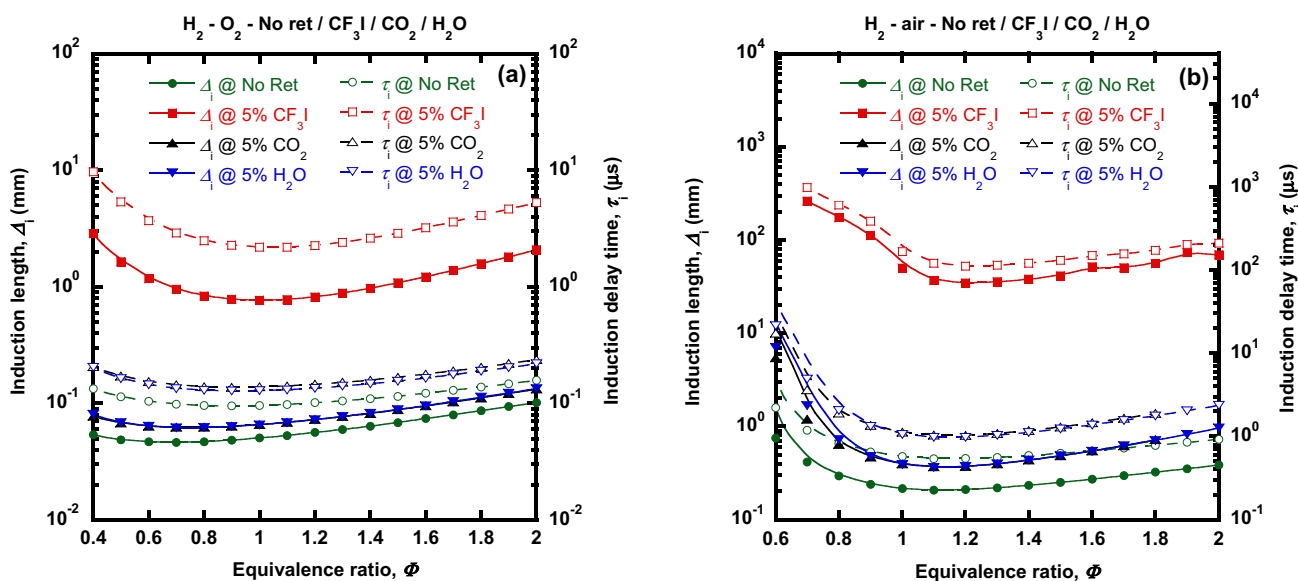
Fig. 2 Effect of varying initial mixture composition on the induction length and time with and without retardants (5% CF₃I, CO₂, and H₂O molar concentration): (**a**) H_2–O_2 detonations and (**b**) H_2–air detonations at $P_0 = 1$ bar and $T_0 = 295$ K

inhibition effect of most halogenated compounds is as follows [39]:

$$H + I + M \rightarrow HI + M \tag{R1}$$

$$I_2 + O \rightarrow I + IO \tag{R2}$$

$$H + CF_3I \rightarrow CF_3 + HI \tag{R3}$$

The above reaction cycle is responsible for the depletion of active radicals H and O in the reaction pool and its corresponding substitution with a less reactive CF_3 radical. The reactions (R1)–(R3) compete with the following conventional chain branching and chain propagation reactions:

$$O_2 + H \rightarrow O + OH \tag{R4}$$

$$H_2 + O \rightarrow H + OH \tag{R5}$$

$$H_2 + OH \rightarrow H + H_2O \tag{R6}$$

and thus produce an inhibition effect on H_2–O_2/air detonations.

The addition of 5% CF₃I to H_2–O_2/air mixtures increases the induction zone length/time for all the equivalence ratios (0.4–2.0). This is because the post-shock temperature, T_{vN}, which governs the chemical kinetics in the induction zone, decreases drastically with the addition of CF₃I. The post-shock temperature without CF₃I for $\Phi = 0.4$, 1.0, and 2.0 is
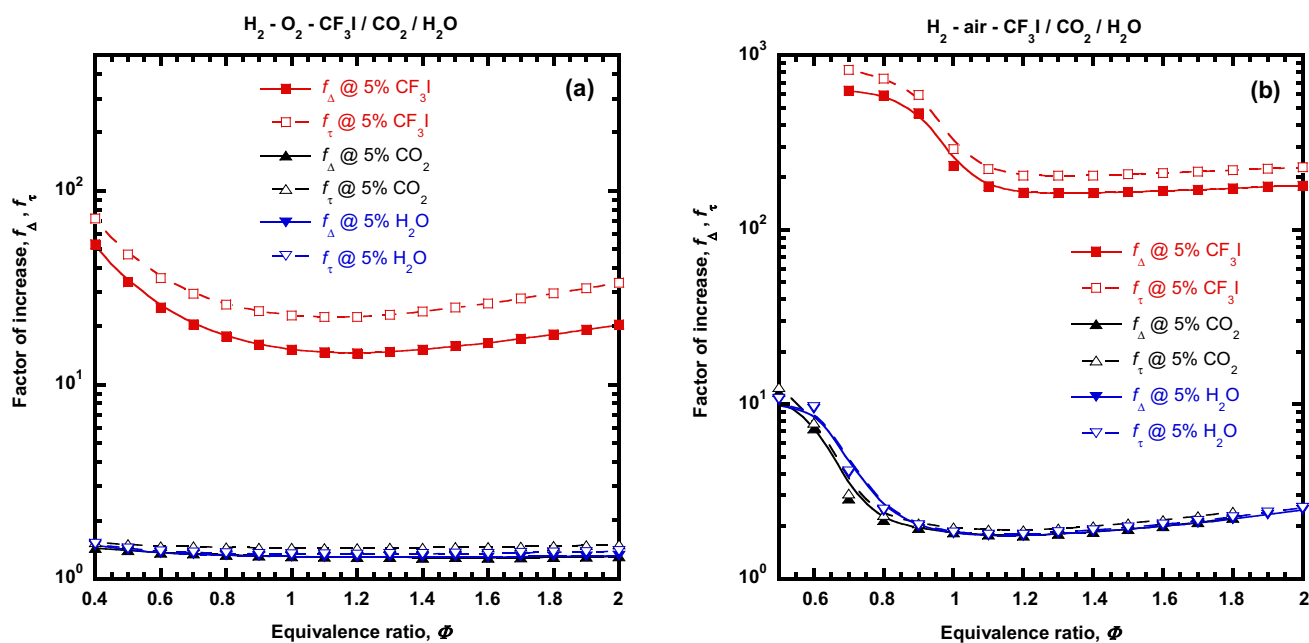
Fig. 3 Effect of varying initial mixture composition on the factor of increase in the induction length (f_Δ) and induction time (f_τ) at 5% CF_3I, CO_2, and H_2O molar concentration: (**a**) H_2–O_2 detonations and (**b**) H_2–air detonations at $P_0 = 1$ bar and $T_0 = 295$ K

1621.6 K, 1761.6 K, and 1724.9 K, respectively, for H_2–O_2 mixtures. However, with the addition of a 5% molar concentration of CF_3I, T_{vN} drops to 1459.1 K, 1605.8 K, and 1545.5 K for $\Phi = 0.4$, 1.0, 2.0, respectively. Similar results can be observed for H_2–air mixtures (refer to Table 1). Thus, the addition of CF_3I decreases T_{vN} substantially, leading to a larger induction length and time. In the case of fuel-lean mixtures, the induction length and time are higher as compared to stoichiometric conditions, and the addition of CF_3I further increases the Δ_i and τ_i. The significant increase in the Δ_i and τ_i for both hydrogen-oxygen/air mixtures with CF_3I addition potentially indicates a very weakly coupled shock-reaction zone, thereby representing a higher probability of a complete decoupling of the shock and the reaction zone. Also, it can be observed that the induction length for H_2–O_2/air–CF_3I mixtures is more than an order of magnitude larger than for H_2–O_2/air–CO_2/H_2O mixtures at the same addition levels. Thus, CF_3I is a far better inhibitor than CO_2 and H_2O at all the equivalence ratios studied.
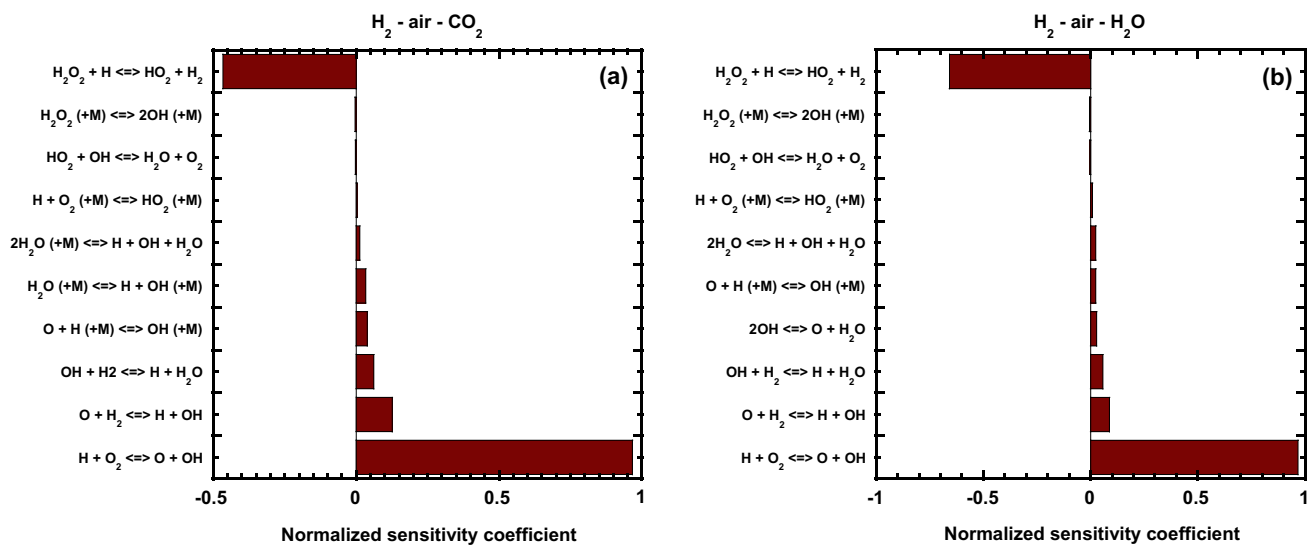
The variation of f_Δ and f_τ with equivalence ratio is illustrated in Fig. 3. The inhibition efficiency varies similarly to the induction length and time with equivalence ratio. It should be noted that the inhibition efficiency of CF_3I is higher in fuel-lean H_2–O_2/air mixtures as compared to stoichiometric and fuel-rich mixtures (refer to Table 1 and Figs. 2 and 3). This is because, in fuel-lean mixtures, the H radicals are present in small amounts. The H-radical is consumed by both the reactions (R3) and (R4). Therefore, the presence of CF_3I hinders the H radical consumption by (R4), thereby

hindering the chain branching process and thus increasing the detonation length and time scales in fuel-lean H_2–O_2/air mixtures. Therefore, higher detonation inhibition efficiency can be observed for CF_3I in fuel-lean conditions due to the limited H radical concentration and competition between hydrogen oxidation and radical scavenging by CF_3I. It can also be observed that with the addition of 5% CF_3I, no detonation was observed at equivalence ratios less than 0.7 (ER < 0.7) for H_2–air–CF_3I mixtures. Thus, it can be concluded that the addition of CF_3I reduces the detonability of a given fuel-air mixture, which is beneficial for hydrogen safety.

3.1.2 H_2–O_2/air–CO_2/H_2O mixtures

The variation in the induction length and time and the inhibition efficiency of CO_2 and H_2O at 5% molar additive concentration were evaluated at various equivalence ratios for H_2–O_2/air–CO_2/H_2O mixtures. Unlike CF_3I, CO_2, and H_2O are known to have an inhibition tendency at all concentrations. Carbon dioxide addition inhibits detonation due to the rapid recombination of the H, O, and OH active radicals with CO and CO_2:

$$CO_2 + O \rightarrow CO + O_2 \tag{R7}$$

$$CO_2 + H \rightarrow OH + CO \tag{R8}$$

$$CO_2 + OH \rightarrow HO_2 + CO \tag{R9}$$

$$O + CO \rightarrow CO_2 \tag{R10}$$

$$H + CO \rightarrow HCO \tag{R11}$$

Fig. 4 Normalized sensitivity coefficients (top ten reactions) for (a) 5% CO_2 and (b) 5% H_2O addition to stoichiometric hydrogen-air mixtures. The initial conditions P_0 and T_0, used for the ZND computations were 1 bar and 295 K, respectively, and the post-shock conditions (P_{vN} and T_{vN}) were used as the initial mixture state for the sensitivity analysis

The consumption of these reactive radicals inhibits the chain branching process and thus increases the induction length and time.

Similarly, H_2O inhibits detonation by removing the active H radical from the reaction pool. However, for H_2O, only the following reaction is critical:

$$H + OH + H_2O \rightarrow 2\,H_2O \tag{R12}$$

in which the H and OH radicals get recombined to form steam (H_2O) [18]. Thus, the reactions (R7)–(R11) for CO_2 and (R12) for H_2O compete with the chain branching and chain propagating reactions (R4)–(R6) and inhibit detonation.

Carbon dioxide and water vapor act like a suppressant or inhibitor over a wide range of fuel-air equivalence ratios, where the induction length steadily increases with the addition of CO_2 and H_2O (see Fig. 2). The post-shock temperature, T_{vN}, also decreases with the addition of CO_2 and H_2O. The decrease in the post-shock temperature is slightly greater for CO_2 than H_2O, but it is substantially less than that for CF_3I. The reduction in the post-shock temperature affects the kinetics in the induction zone and governs the induction zone length and time. Thus, CO_2 and H_2O are comparable inhibitors at all the equivalence ratios but are inferior to CF_3I as the increase in Δ_i is higher for CF_3I than CO_2 and H_2O under the conditions tested.

In order to gain insights into the underlying reaction kinetics, temperature sensitivity analysis was performed for stoichiometric hydrogen-air detonations in the presence of 5% CO_2 and H_2O. The initial conditions for the computations were the corresponding post-shock thermodynamic state ((a)

CO_2: $P_{vN} = 26.9$ bar, and $T_{vN} = 1438.1$ K; (b) H_2O: $P_{vN} = 27.15$ bar, and $T_{vN} = 1480.4$ K). It can be seen that the addition of CO_2 and H_2O results in similar sensitivity spectra under the given conditions. The primary chain branching reaction, H + O_2 $\leftrightarrow$ O + OH exhibits the highest positive sensitivity coefficient. A slight increase in the reaction rate of this reaction can significantly increase the temperature (in the reaction zone), leading to lower induction zone length/time for both H_2–air–CO_2/H_2O mixtures. The reactions that exhibit a positive sensitivity coefficient are mostly chain branching or chain propagating in nature, as shown in Fig. 4. It must be observed that the reactions responsible for the inhibition effect of carbon dioxide (R7)–(R11) and steam (R12) are not among the ten most influential reactions for the given mixture under detonating conditions. Thus, it can be concluded that the inhibition effect observed for CO_2 and H_2O when added to hydrogen-air mixtures is primarily due to the change in the post-shock temperature, T_{vN}, and the chemical reaction cycle plays a secondary role under the conditions tested.

The inhibition efficiency of CO_2 and H_2O remains relatively constant for H_2–O_2–CO_2/H_2O mixtures at all the equivalence ratios, as shown in Table 1 and Fig. 3a. However, for H_2–air–CO_2/H_2O mixtures, the inhibition efficiency is comparatively higher at fuel-lean conditions than at fuel-rich conditions. In the case of H_2–air–CO_2/H_2O mixtures, the factor of increase in the induction length (f_Δ) at $\Phi = 0.6$ is ~7.3 and ~9.4, and at $\Phi = 1.6$, it is ~2 and ~1.9 for CO_2 and H_2O respectively. Thus, H_2O has a better inhibiting ability for H_2–air detonations at off-stoichiometric fuel-lean conditions.

Table 2 Critical detonation parameters (T_{vN}, Δ_i, and τ_i) and the factor of increase (f_Δ, f_τ) at various mixture initial pressure (P_0) with and without inhibitors for H_2–O_2/air mixtures

	P_0 (bar)	H_2–O_2					H_2–air				
		T_{vN} (K)	Δ_i (mm)	τ_i (µs)	f_Δ	f_τ	T_{vN} (K)	Δ_i (mm)	τ_i (µs)	f_Δ	f_τ
No inhibitor	0.2	1677.9	0.308	0.602	–	–	1492.0	1.070	2.904	–	–
	1.0	1761.7	0.050	0.096	–	–	1535.4	0.215	0.573	–	–
	5.0	1846.4	0.011	0.021	–	–	1572.8	0.124	0.328	–	–
5% CF$_3$I	0.2	1539.2	4.94	14.69	16.1	24.4	1305.6	224.5	763.7	209.7	263.0
	1.0	1605.8	0.76	2.18	15.2	22.8	1326.3	50.2	166.7	233.2	290.8
	5.0	1670.9	0.13	0.36	11.8	17.5	1341.5	11.4	37.4	91.3	113.9
5% CO$_2$	0.2	1600.4	0.379	0.818	1.23	1.36	1403.2	1.57	4.53	1.46	1.56
	1.0	1674.8	0.066	0.138	1.31	1.44	1438.0	0.40	1.13	1.84	1.96
	5.0	1749.6	0.020	0.040	1.74	1.94	1468.0	0.47	1.34	3.77	4.07
5% H$_2$O	0.2	1634.9	0.367	0.739	1.19	1.23	1443.3	1.42	3.89	1.32	1.34
	1.0	1712.3	0.065	0.128	1.30	1.3	1480.3	0.39	1.06	1.81	1.84
	5.0	1790.3	0.021	0.040	1.87	1.9	1511.2	0.40	1.08	3.22	3.29

The inhibition efficiency of the inhibitors CF$_3$I, CO$_2$, and H$_2$O varies considerably with the fuel-oxidizer equivalence ratio, specifically for fuel-air-inhibitor mixtures. It can be concluded that the variation in the inhibition efficiency is the result of two separate governing parameters: the post-shock temperature, T_{vN}, which changes with the addition of inhibitor, and the radical abstraction mechanism of the inhibitors, which can be quantified by evaluating the maximum H-concentration.

3.2 Effect of varying initial pressure on the inhibition efficiency

3.2.1 H$_2$–O$_2$/air–CF$_3$I mixtures

The induction length decreases with an increase in initial mixture pressure from 0.2 bar to 5 bar at the stoichiometric condition with and without any additives or inhibitors, as shown in Table 2 and Fig. 5a and b. The addition of CF$_3$I to H$_2$–O$_2$ and H$_2$–air mixtures increases the induction length due to the suppression or inhibition effect at any pressure (refer to Table 2 and Fig. 5). Although the addition of inhibitors offers an inhibiting effect for most H$_2$–O$_2$ and H$_2$–air mixtures at any pressure, the inhibition efficiency or the factor of increase in the induction length and time decreases with increasing pressure. This is shown in Fig. 6a and b for CF$_3$I -diluted stoichiometric H$_2$–O$_2$ and H$_2$–air mixtures. For example, the addition of 5% CF$_3$I at an initial pressure of 0.6 bar increases the induction length for a stoichiometric hydrogen-oxygen mixture by a factor of ~15.4 compared to the case with no CF$_3$I. However, for the same concentration at a higher initial pressure of 5 bar, the induction length increases by ~11.8 compared to the case with no CF$_3$I. Similarly, the addition of 5% CF$_3$I at an initial

pressure of 0.6 bar increases the induction zone length for a stoichiometric hydrogen-air mixture by a factor of ~235 compared to the case with no CF$_3$I. However, for the same concentration at a higher initial pressure of 5 bar, the induction length increases by a factor of ~91 compared to the case with no CF$_3$I. Thus, the inhibition efficiency of CF$_3$I seems to decrease with increasing pressure, but still, CF$_3$I is a far better inhibitor than CO$_2$ and H$_2$O.

At higher initial pressures, the recombination reaction

$$O_2 + H (+ M) \rightarrow HO_2 (+M) \tag{R13}$$

competes with the branching reaction

$$O_2 + H \rightarrow OH + O \tag{R14}$$

It causes an increase in the induction length and time scales due to a decrease in the radical pool concentration. Since detonations are already inhibited by the effects of this competition for H atoms, the addition of CF$_3$I does not have a more significant impact on the Δ_i and τ_i as the pressure is increased.

Therefore, the inhibition efficiency decreases with increasing initial pressure for a particular concentration of an inhibitor like CF$_3$I. The effect of mixture initial pressure on the Δ_i and τ_i is similar for both H$_2$–O$_2$–CF$_3$I and H$_2$–air–CF$_3$I mixtures. The same is true for H$_2$–O$_2$ and H$_2$–air mixtures without any inhibitors.

3.2.2 H$_2$–O$_2$/air–CO$_2$/H$_2$O mixtures

The addition of CO$_2$ and H$_2$O diluents or inhibitors to H$_2$–O$_2$ and H$_2$–air mixtures increases the induction length for constant P_0 and T_0. Thus, the increase in the Δ_i and τ_i
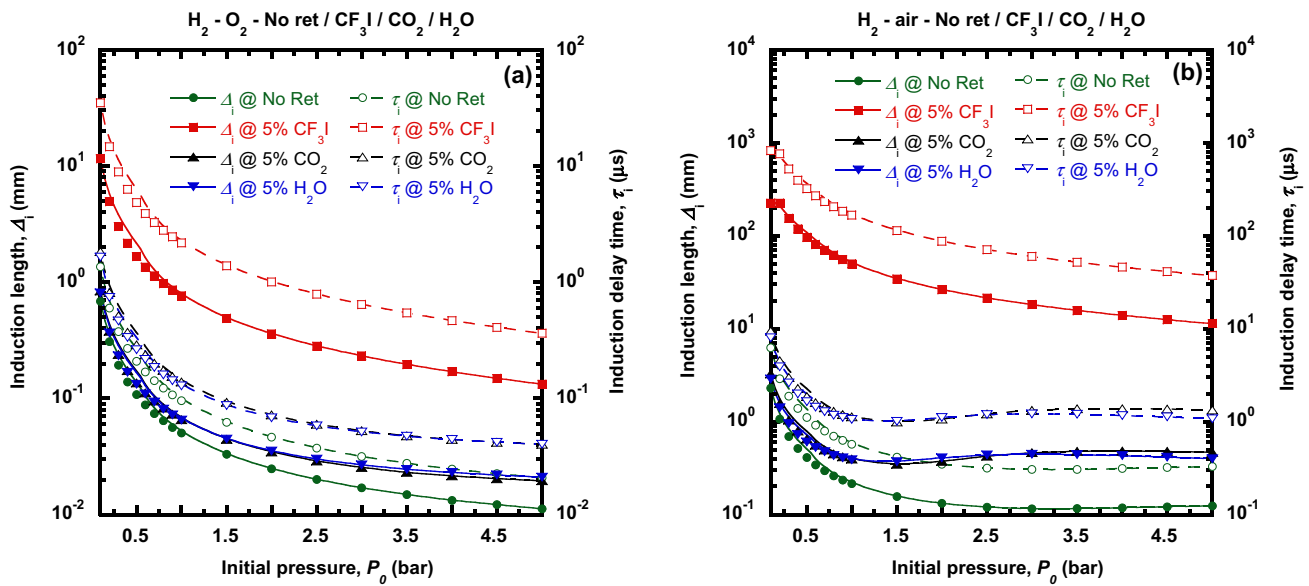
Fig. 5 Effect of varying initial mixture pressure on the induction length and time with and without inhibitors (5% CF$_3$I, CO$_2$, and H$_2$O molar concentration): (**a**) H$_2$–O$_2$ detonations and (**b**) H$_2$–air detonations at $\Phi = 1$ and $T_0 = 295$ K
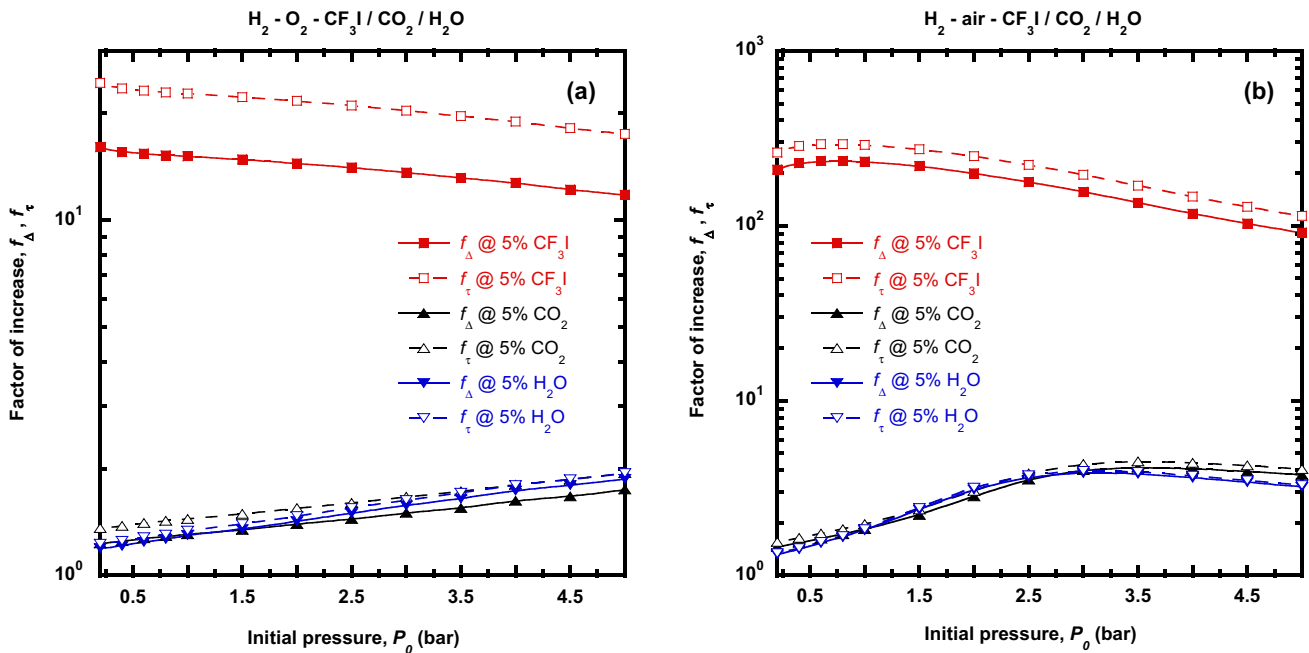

Fig. 6 Effect of varying initial mixture pressure on the factor of increase in the induction length (f_Δ) and induction time (f_τ) at 5% CF$_3$I, CO$_2$, and H$_2$O molar concentration: (**a**) H$_2$–O$_2$ detonations and (**b**) H$_2$–air detonations at $\Phi = 1$ and $T_0 = 295$ K

reduces the detonability and, in turn, the detonation hazard for CO$_2$/H$_2$O diluted H$_2$–O$_2$/air mixtures. The addition of CO$_2$ and H$_2$O provides an inhibiting effect for hydrogen-oxygen and hydrogen-air mixtures at any pressure. Also, the inhibiting efficiency of these inhibitors increases rapidly with increasing pressure. This is shown in Figs. 5 and 6 for CO$_2$-diluted and H$_2$O-diluted stoichiometric H$_2$–O$_2$ and H$_2$–air mixtures at $T_0 = 295$ K. For example, the addition

of 5% CO$_2$ at an initial pressure of 0.2 bar increases the induction zone length for a stoichiometric hydrogen-oxygen mixture by a factor of ~1.23 compared to the case with no CO$_2$. However, for the same dilution levels of CO$_2$ at a higher initial pressure of 5 bar, the induction length increases by a factor of ~1.75 compared to the case with no CO$_2$.

Similarly, the addition of 5% CO$_2$ at an initial pressure of 0.2 bar increases the induction zone length for a stoichio-

Table 3 Critical detonation parameters (T_{vN}, Δ_i, and τ_i) and the factor of increase (f_Δ, f_τ) at various mixture initial temperatures (T_0) with and without inhibitors for H_2–O_2/air mixtures

	T_0 (K)	H_2–O_2					H_2–air				
		T_{vN} (K)	Δ_i (mm)	τ_i (µs)	f_Δ	f_τ	T_{vN} (K)	Δ_i (mm)	τ_i (µs)	f_Δ	f_τ
No inhibitor	300	1764.1	0.051	0.097	–	–	1538.7	0.215	0.572	–	–
	500	1871.2	0.071	0.125	–	–	1671.7	0.236	0.575	–	–
	1000	2171.6	0.106	0.156	–	–	2015.2	0.288	0.589	–	–
5% CF_3I	300	1608.6	0.75	2.15	14.8	22.3	1330.2	48.96	162.29	227.5	283.6
	500	1727.5	0.33	0.88	4.7	7.0	1484.7	13.32	41.59	56.4	72.3
	1000	2059.4	0.09	0.21	0.9	1.3	1876.8	0.73	1.95	2.5	3.4
5% CO_2	300	1677.3	0.066	0.139	1.30	1.44	1441.4	0.388	1.104	1.80	1.93
	500	1787.8	0.085	0.166	1.21	1.33	1578.0	0.332	0.858	1.40	1.49
	1000	2098.4	0.120	0.193	1.13	1.24	1932.8	0.351	0.726	1.22	1.28
5% H_2O	300	1715.9	0.066	0.128	1.29	1.33	1483.5	0.384	1.037	1.78	1.81
	500	1824.5	0.084	0.153	1.19	1.22	1619.4	0.310	0.762	1.31	1.33
	1000	2127.2	0.121	0.182	1.14	1.17	1967.2	0.336	0.668	1.17	1.18

metric hydrogen-air mixture by a factor of ~1.46 compared to the case with no CO_2. However, for the same dilution at a higher initial pressure of 5 bar, the induction length increases significantly by a factor of ~3.8 compared to the case without CO_2. For mixtures diluted with H_2O, the addition of 5% H_2O at an initial pressure of 0.2 bar increases the induction zone length for a stoichiometric hydrogen-oxygen mixture by a factor of ~1.2 compared to the case with no steam. However, for the same dilution levels of steam at a higher initial pressure of 5 bar, the induction length increases significantly by a factor of ~1.9 compared to the case with no steam. Similar results were obtained for stoichiometric hydrogen-air mixtures. Thus, when compared with the no-inhibitor case, the inhibitors seem to have increased inhibition efficiency with increasing pressure (refer to Table 2 and Fig. 6a and b).

The addition of CO_2 and H_2O inhibitors to stoichiometric hydrogen-air mixtures increases the induction length and time at pressures greater than 1 bar ($P_0 > 1$ bar). However, at very low pressures, the induction zone lengths seem to approach each other with the addition of CO_2 and H_2O, see Fig. 5b. The computational results also exhibit a local minimum in the induction length with increasing initial pressure. The increase in initial pressure in the presence of inhibitors like CO_2 and H_2O would decrease the induction length initially and attain a minimum. After minima, the induction length increases with an increase in initial pressure, as shown in Fig. 5b. However, this effect is primarily seen in H_2–air–CO_2/H_2O mixtures and not in H_2–O_2–CO_2/H_2O mixtures. The results are consistent with the literature where Stamps and Tieszen observed a cell width minimum in H_2O-diluted hydrogen-air detonations [23].

## 3.3 Effect of varying initial temperature on the inhibition efficiency

3.3.1 H_2–O_2/air–CF_3I mixtures

Hydrogen-oxygen and hydrogen-air mixtures with CF_3I have larger induction zone lengths than those without CF_3I addition. However, it can be observed that the induction length and time for CF_3I diluted H_2–O_2/air mixtures decrease with an increase in the initial temperature. In contrast, the induction length and time increase for CO_2 and H_2O diluted H_2–O_2/air mixtures (refer to Table 3). Although the addition of CF_3I increases the induction length and time (compared to the no inhibitor case) and offers an inhibiting effect for most hydrogen-oxygen and hydrogen-air mixtures at all mixture temperatures, the inhibiting effect decreases rapidly with increasing temperature. This is shown in Figs. 7 and 9 for CF_3I-diluted stoichiometric H_2–O_2 and H_2–air mixtures at $P_0 = 1$ bar.

For example, the addition of 5% CF_3I increases the induction zone length for a stoichiometric hydrogen-oxygen mixture by a factor of ~14.8 at 300 K compared to the case with no CF_3I. However, the induction length decreases for the same concentration level at a higher initial temperature of 1000 K compared to the case with no CF_3I. Similarly, the addition of 5% CF_3I at an initial temperature of 300 K increases the induction zone length for a stoichiometric hydrogen-air mixture by a factor of ~227.5 compared to the case with no CF_3I. Again, for the same concentration level at a higher initial temperature of 1000 K, the induction length increases by ~2.5 compared to the case with no CF_3I. Thus, the impact of the initial temperature on the induction zone length and time is similar for both H_2–O_2–CF_3I and H_2–
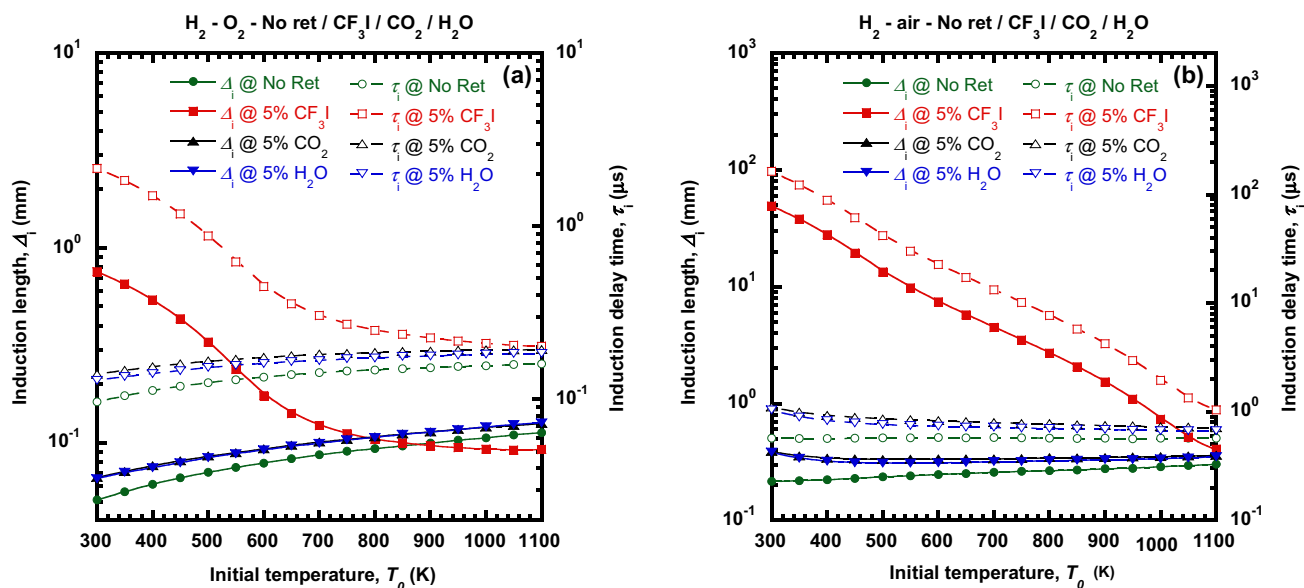
Fig. 7 Effect of varying initial mixture temperature on the induction length and time with and without retardants (5% CF_3I, CO_2, and H_2O molar concentration): (**a**) H_2–O_2 detonations and (**b**) H_2–air detonations at $\Phi = 1$ and $P_0 = 1$ bar
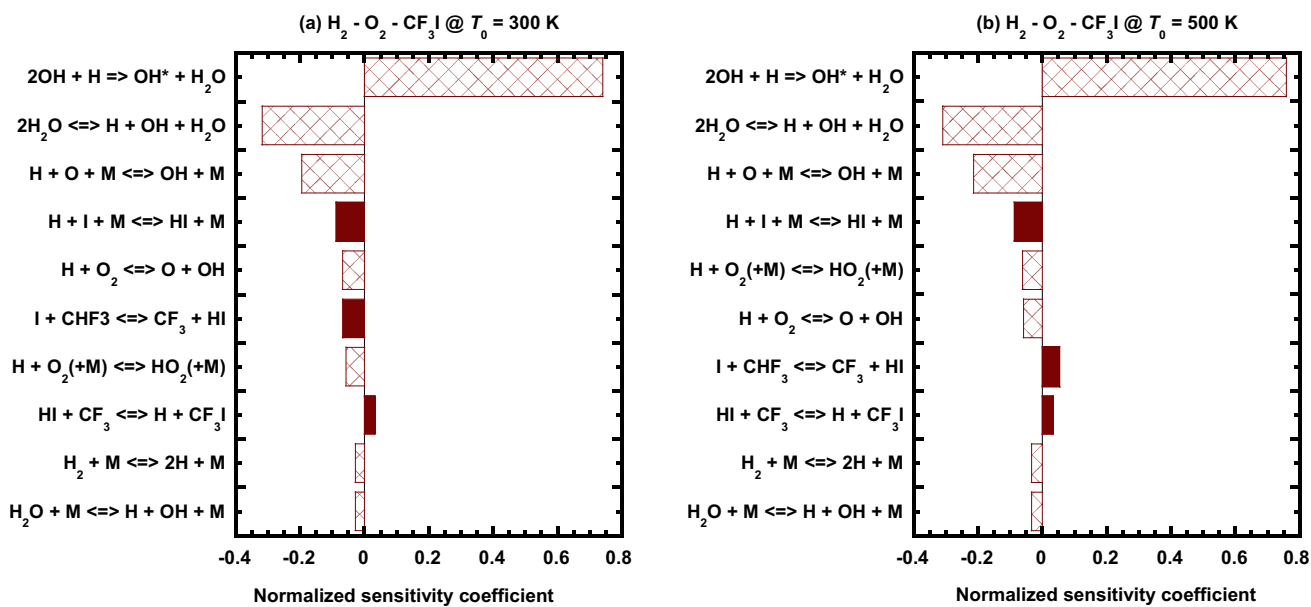

Fig. 8 Normalized sensitivity coefficients (top ten reactions) for stoichiometric H_2–O_2–CF_3I (5%) mixtures at (**a**) $T_0 = 300$ K and (**b**) $T_0 = 500$ K. The initial conditions for the sensitivity computations were the corresponding post-shock conditions (P_{vN} and T_{vN}). Reactions that belong to the CF_3I sub-mechanism are marked as solid color bars

air–CF_3I mixtures, where the inhibiting efficiency of CF_3I was found to decrease rapidly with increasing temperature. The effect of the mixture's initial temperature on the induction length is quite different for H_2–O_2/air mixtures and H_2–O_2/air–CF_3I mixtures. For example, the induction length increases with an increase in initial temperature from 300 to 1100 K for hydrogen-oxygen/air mixtures in the absence of CF_3I. However, for hydrogen-oxygen/air–CF_3I mixtures, the

induction length decreases with an increase in initial temperature from 300 to 1100 K.

The decrease in the inhibition effectiveness of CF_3I at higher temperatures is an interesting result, as the inhibition effectiveness of CO_2 and H_2O remains relatively constant with changes in initial temperature. In order to evaluate the dominant reactions responsible for the observed effect, temperature sensitivity analysis was carried out for
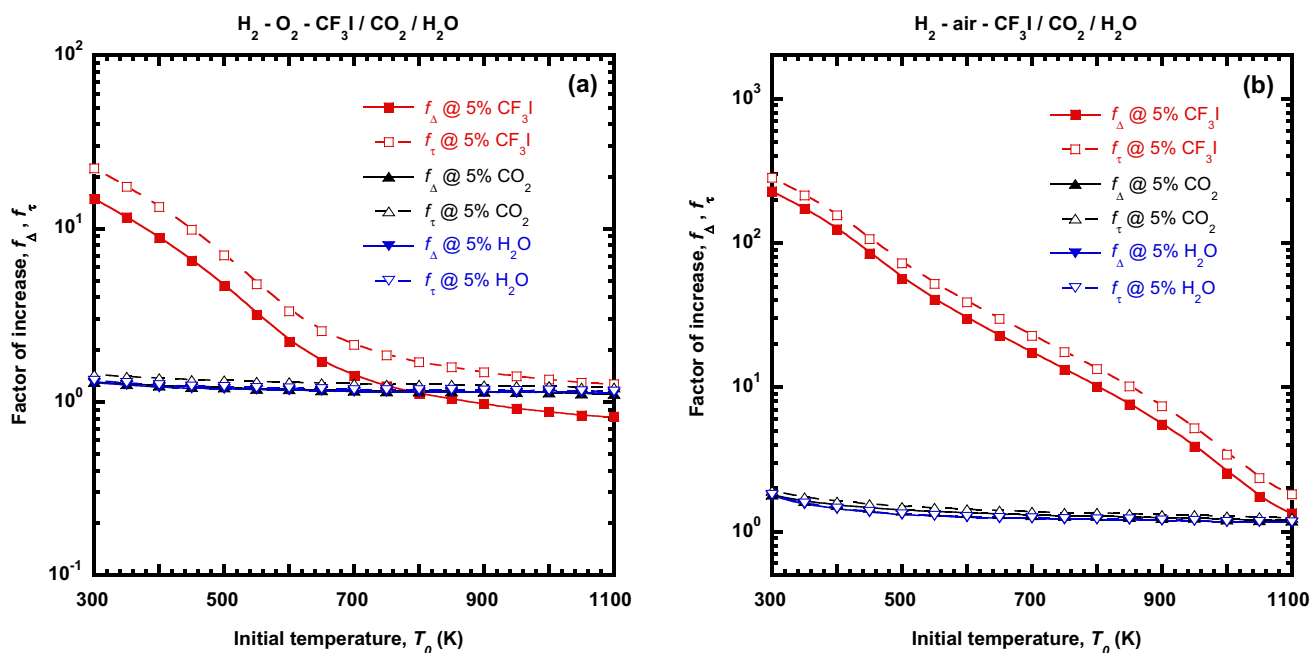
Fig. 9 Effect of varying initial mixture temperature on the factor of increase in the induction length (f_Δ) and induction time (f_τ) at 5% CF$_3$I, CO$_2$, and H$_2$O molar concentration: (**a**) H$_2$–O$_2$ detonations and (**b**) H$_2$–air detonations at $\Phi = 1$ and $P_0 = 1$ bar

H$_2$–O$_2$–CF$_3$I mixtures at different initial temperatures. The initial conditions for the sensitivity computations were the corresponding post-shock states ((a) $T_0 = 300$ K: $P_{vN} = 32.4$ bar, and $T_{vN} = 1608.6$ K; (b) $T_0 = 500$ K: $P_{vN} = 18.8$ bar, and $T_{vN} = 1727.5$ K). The normalized sensitivity coefficients for the top ten reactions are shown in Fig. 8. It can be observed that the consumption of H radical through the reaction H + I + M $\leftrightarrow$ HI + M shows the highest negative sensitivity coefficient (amongst reactions belonging to the CF$_3$I sub-mechanism). The reaction is responsible for an increase in the induction length with the addition of CF$_3$I, irrespective of the initial mixture temperature. At $T_0 = 300$ K (Fig. 8a), the reaction CHF$_3$ + I $\leftrightarrow$ CF$_3$+HI exhibits a negative sensitivity coefficient, thereby contributing to the inhibition effect. However, as the initial temperature is increased to $T_0 = 500$ K (Fig. 8b), the reaction exhibits a positive sensitivity coefficient. The production of H radical through the combined effect of the reactions, CHF$_3$ + I $\leftrightarrow$ CF$_3$ + HI and CF$_3$ + HI $\leftrightarrow$ CF$_3$I+ H results in radical proliferation, thereby reducing the induction length for H$_2$ – O$_2$ – CF$_3$I mixtures at elevated temperatures. Thus, the inhibition effectiveness of CF$_3$I diminishes at higher initial temperatures due to the change in sensitivities of the elementary reactions to the initial conditions.

3.3.2 H$_2$–O$_2$/air–CO$_2$/H$_2$O mixtures

H$_2$–O$_2$ and H$_2$–air mixtures diluted with CO$_2$ and H$_2$O have larger induction zone lengths than the same mixture without dilution. The addition of CO$_2$ and H$_2$O inhibits H$_2$–O$_2$/air detonations; however, it can be seen from Fig. 9a and b that the inhibition efficiency of these inhibitors is minimally affected with an increase in the initial temperature of the reacting mixture, unlike CF$_3$I diluted stoichiometric H$_2$–O$_2$ and H$_2$–air mixtures. For example, the addition of 5% CO$_2$ at an initial temperature of 300 K increases the induction zone length for a stoichiometric hydrogen-oxygen mixture by a factor of ~1.3 compared to the case with no CO$_2$. However, for the same dilution at a higher initial temperature of 1000 K, the induction length increases by only a factor of ~1.1.

This represents that the inhibition efficiency of CO$_2$ decreases slightly with the rise in initial temperature. For mixtures diluted with steam, the addition of 5% H$_2$O at an initial temperature of 300 K increases the induction zone length for a stoichiometric hydrogen-oxygen mixture by a factor of ~1.3 compared to the case with no steam. However, at a higher initial temperature of 1000 K, the induction length increases only by a factor of ~1.1. Similarly, the addition of 5% H$_2$O at an initial temperature of 300 K increases the induction zone length for a stoichiometric hydrogen-air

mixture by a factor of ~1.8 compared to the case with no H$_2$O. However, the same amount of dilution at a higher initial temperature of 1000 K increases the induction length by only a factor of ~1.2 (refer to Table 3). Thus, the inhibition efficiency of H$_2$O decreases with an increase in the initial temperature.

The addition of CO$_2$/H$_2$O seems to have quite a different effect for H$_2$–O$_2$ and H$_2$–air mixtures. The addition of CO$_2$/H$_2$O increases the induction zone length in the case of H$_2$–O$_2$ mixtures, whereas the induction length remains mostly constant for H$_2$–air mixtures. Therefore, at a higher mixture initial temperature, CO$_2$ and H$_2$O are as good inhibitors as CF$_3$I and thus can be used for detonation inhibition under the conditions studied.

4 Conclusions

The efficiency of detonation inhibitors on H$_2$–O$_2$/air detonations was evaluated under varying mixture initial conditions using numerical computations. The inhibitors CF$_3$I, CO$_2$, and H$_2$O at 5% molar concentration were added to H$_2$–O$_2$/air mixtures, and the factor of increase in the induction zone length and time was used as an indicative parameter of the inhibition efficiency of the detonation inhibitors. It was found that CF$_3$I is a far better inhibitor than CO$_2$ and H$_2$O at all the mixture equivalence ratios studied in the current work. The inhibition efficiency of CF$_3$I is higher in fuel-lean H$_2$–O$_2$/air mixtures than in stoichiometric and fuel-rich mixtures. The addition of CF$_3$I drastically reduces the detonability of a given fuel-air mixture. It was also found that CO$_2$ and H$_2$O have a comparable inhibition efficiency at all the equivalence ratios but are inferior to CF$_3$I in inhibiting a detonation wave under similar initial mixture conditions. In comparison to CO$_2$, H$_2$O has a better inhibiting ability for H$_2$–air detonations at off-stoichiometric fuel-lean conditions. The inhibition efficiency was found to be the result of two separate governing parameters: the post-shock temperature, T_{vN} which changes with the addition of an inhibitor and the radical abstraction mechanism of the inhibitors. The inhibiting efficiency of CF$_3$I was found to decrease with increasing initial mixture pressure; however, it was still a better inhibitor when compared with CO$_2$ and H$_2$O. On the other hand, the inhibition efficiency of CO$_2$ and H$_2$O increased rapidly with increasing mixture pressure. At very low initial pressures, the induction zone lengths approached each other with the addition of CO$_2$ and H$_2$O as inhibitors. The variation of induction length with initial mixture temperature showed an interesting behavior where it decreases for H$_2$–O$_2$/air–CF$_3$I mixtures and increases for undiluted and H$_2$–O$_2$/air–CO$_2$/H$_2$O mixtures. The inhibition efficiency of CO$_2$ and H$_2$O is minimally affected with an increase in the initial temperature. A key takeaway from the current study is the effect of initial tem-

perature on the inhibition efficiency of CF$_3$I. It was found that the efficiency decreased drastically at a higher mixture initial temperature. This result is of particular importance for flame and detonation suppression in nuclear reactors where the initial flammable mixture temperature is higher, and the results from the current findings can be used to make a proper choice of inhibitor under such conditions.

The inhibiting effect of detonation inhibitors varied drastically with the initial conditions, and the same should be taken into consideration while designing fire and detonation safety systems for applications in petrochemical industries and nuclear reactors. It should be noted that for all the inhibitors studied, the inhibition efficiency is minimal at very high initial temperatures. The current study on H$_2$–O$_2$/air detonating mixtures lays the groundwork for further studies on detonation inhibition in hydrocarbon-O$_2$/air mixtures and scenarios for possible gas leaks leading to vapor cloud formation, especially under confined spaces.

References

1. Wang, L., Ma, H., Shen, Z., Pan, J.: A comparative study of the explosion behaviors of H$_2$ and C$_2$H$_4$ with air, N$_2$O, and O$_2$. Fire Saf. J. **119**(1), 103260 (2021). https://doi.org/10.1016/j.firesaf.2020.103260

2. Crowl, D.A., Jo, Y.: The hazards and risks of hydrogen. J. Loss Prev. Process Ind. **20**(1), 158–164 (2007). https://doi.org/10.1016/j.jlp.2007.02.002

3. Rosyid, O.A., Jablonski, D., Hauptmanns, U.: Risk analysis for the infrastructure of a hydrogen economy. Int. J. Hydrogen Energy **32**(15), 3194–3200 (2007). https://doi.org/10.1016/j.ijhydene.2007.02.012

4. Thomas, J.K., Eastwood, C., Goodrich, M.: Are unconfined hydrogen vapor cloud explosions credible? Process Saf. Prog. **34**(1), 36–43 (2014). https://doi.org/10.1002/prs.11685

5. Kim, W.K., Mogi, T., Dobashi, R.: Fundamental study on accidental explosion behavior of hydrogen-air mixtures in an open space. Int. J. Hydrogen Energy **38**(19), 8024–8029 (2013). https://doi.org/10.1016/j.ijhydene.2013.03.101

6. Oran, E.S.: Understanding explosions - From catastrophic accidents to the creation of the universe. Proc. Combust. Inst. **35**(1), 1–35 (2015). https://doi.org/10.1016/j.proci.2014.08.019

7. Oran, E.S., Gamezo, V.N.: Origins of the deflagration-to-detonation transition in gas-phase combustion. Combust. Flame **148**(1–2), 4–47 (2007). https://doi.org/10.1016/j.combustflame.2006.07.010

8. Oran, E.S., Chamberlain, G., Pekalski, A.: Mechanisms and occurrence of detonations in vapor cloud explosions. Prog. Energy Combust. Sci. **77**(1), 100804 (2020). https://doi.org/10.1016/j.pecs.2019.100804

9. Jiang, Y., Li, Y., Zhou, Y., Jiang, H., Zhang, K., Gao, Z., Gao, W.: Investigation on unconfined hydrogen cloud explosion with external turbulence. Int. J. Hydrogen Energy **47**(13), 8658–8670 (2022). https://doi.org/10.1016/j.ijhydene.2021.12.167

10. Machniewski, P., Molga, E.: CFD analysis of large-scale hydrogen detonation and blast wave overpressure in partially confined spaces. Process Saf. Environ. Prot. **158**(1), 537–546 (2022). https://doi.org/10.1016/j.psep.2021.12.032

11. Palacios, A., Bradley, D.: Hydrogen generation, and its venting from nuclear reactors. Fire Saf. J. **113**(1), 102968 (2020). https://doi.org/10.1016/j.firesaf.2020.102968

12. Westbrook, C.K.: Inhibition of hydrocarbon oxidation in laminar flames and detonations by halogenated compounds. Proc. Combust. Inst. **19**(1), 127–141 (1982). https://doi.org/10.1016/S0082-0784(82)80185-9

13. Van Tiggelen, P.J., Lefebvre, M.H.: Flame retardants effectiveness in gaseous detonation mitigation. Proceedings of Halon Options Technical Working Conference, Albuquerque, NM, May 12–14 (1998)

14. Leclerc, B.F., Glaude, P.A., Come, G.M., Baronnet, F.: Inhibiting effect of CF$_3$I on the reaction between CH4 and O2 in a jet-stirred reactor. Combust. Flame **103**(3), 285–292 (1997). https://doi.org/10.1016/S0010-2180(96)00168-X

15. Mathieu, O., Goulier, J., Gourmel, F., Mannan, M.S., Chaumeix, N., Petersen, E.L.: Experimental study of the effect of CF$_3$I addition on the ignition delay time and laminar flame speed of methane, ethylene, and propane. Proc. Combust. Inst. **35**(3), 2731–2739 (2015). https://doi.org/10.1016/j.proci.2014.05.096

16. Moen, I.O., Ward, S.A., Thibault, P.A., Lee, J.H.S., Knystautas, R., Dean, T., Westbrook, C.K.: The influence of diluents and inhibitors on detonations. Proc. Combust. Inst. **20**(1), 1717–1725 (1985). https://doi.org/10.1016/S0082-0784(85)80668-8

17. Zhang, C., Wen, J., Shen, X., Xiu, G.: Experimental study of hydrogen/air premixed flame propagation in a closed channel with inhibitions for safety consideration. Int. J. Hydrogen Energy **44**(40), 22654–22660 (2019). https://doi.org/10.1016/j.ijhydene.2019.04.032

18. Kumar, D.S., Singh, A.V.: Inhibition of hydrogen-oxygen/air gaseous detonations using CF$_3$I, H$_2$O, and CO$_2$. Fire Saf. J. **124**(1), 103405 (2021). https://doi.org/10.1016/j.firesaf.2021.103405

19. Drakon, A.V., Eremin, A.V., Mikheyeva, E.Y.: On chemical inhibition of shock wave ignition of hydrogen-oxygen mixtures. J. Phys. Conf. Ser. **946**(1), 012062 (2018). https://doi.org/10.1088/1742-6596/946/1/012062

20. Evariste, F., Lefebre, M.H., Van Tiggelen, P.J.: Inhibition of detonation wave with halogenated compounds. Shock Waves **6**(1), 233–239 (1996). https://doi.org/10.1007/BF02511380

21. Babushok, V., Noto, T., Burgess, D.R.F., Hamins, A., Tsang, W.: Influence of CF3I, CF3Br, and CF3H on the high-temperature combustion of methane. Combust. Flame **107**(4), 351–367 (1996). https://doi.org/10.1016/S0010-2180(96)00052-1

22. Noto, T., Babushok, V., Hamins, A., Tsang, W.: Inhibition effectiveness of halogenated compounds. Combust. Flame **112**(1–2), 147–160 (1998). https://doi.org/10.1016/S0010-2180(97)81763-4

23. Stamps, D.W., Tieszen, S.R.: The influence of initial pressure and temperature on hydrogen-air-diluent detonations. Combust. Flame **83**(1), 353–364 (1991). https://doi.org/10.1016/0010-2180(91)90082-M

24. Lee, J.H.S.: The Detonation Phenomenon. Cambridge University Press, Cambridge (2008)

25. Vasil'ev, A.A.: Cell size as the main geometric parameter of a multifront detonation wave. J. Propul. Power **22**(6), 1245–1260 (2012). https://doi.org/10.2514/1.20348

26. Tieszen, S.R., Stamps, D.W., Westbrook, C.K., Pitz, W.J.: Gaseous hydrocarbon-air detonations. Combust. Flame **84**(3–4), 367–390 (1991). https://doi.org/10.1016/0010-2180(91)90013-2

27. Ciccarelli, G., Ginsberg, T., Boccio, J., Economos, C., Kinoshita, M.: Detonation cell size measurements and predictions in hydrogen-air-steam mixtures at elevated temperatures. Combust. Flame **99**(2), 212–220 (1994). https://doi.org/10.1016/0010-2180(94)90124-4

28. Stamps, D.W., Slezak, S.E., Tieszen, S.R.: Observations of the cellular structure of fuel-air detonations. Combust. Flame **144**(1–2), 289–298 (2006). https://doi.org/10.1016/j.combustflame.2005.06.016

29. Gavrikov, A.I., Efimenko, A.A., Dorofeev, S.B.: A model for detonation cell size prediction from chemical kinetics. Combust. Flame **120**(1), 19–33 (2000). https://doi.org/10.1016/S0010-2180(99)00076-0

30. Shepherd, J.E.: Chemical kinetics of hydrogen-air-diluent detonations. Prog. Astronaut. Aeronaut. **106**(1), 263–293 (1986). https://doi.org/10.2514/5.9781600865800.0263.0293

31. Westbrook, C.K., Urtiew, P.A.: Chemical kinetic prediction of critical parameters in gaseous detonations. Proc. Combust. Inst. **19**(1), 615–623 (1982). https://doi.org/10.1016/S0082-0784(82)80236-1

32. Crane, J., Shi, X., Singh, A.V., Tao, Y., Wang, H.: Isolating the effect of induction length on detonation structure: Hydrogen-oxygen detonation promoted by ozone. Combust. Flame **200**(1), 44–52 (2018). https://doi.org/10.1016/j.combustflame.2018.11.008

33. Ng, H., Ju, Y., Lee, J.: Assessment of detonation hazards in high-pressure hydrogen storage from chemical sensitivity analysis. Int. J. Hydrogen Energy **32**(1), 93–99 (2007). https://doi.org/10.1016/j.ijhydene.2006.03.012

34. Mével, R., Lafosse, F., Catoire, L., Chaumeix, N., Dupré, G., Paillard, C.-E.: Induction delay times and detonation cell size prediction of hydrogen-nitrous oxide-diluent mixtures. Combust. Sci. Technol. **180**(10–11), 1858–1875 (2008). https://doi.org/10.1080/00102200802261340

35. Zhang, B., Ng, H.D., Mével, R., Lee, J.H.S.: Critical energy for direct initiation of spherical detonations in H2/N2O/Ar mixtures. Int. J. Hydrogen Energy **36**(1), 5707–5716 (2011). https://doi.org/10.1016/j.ijhydene.2011.01.175

36. Browne, S., Ziegler, J., Bitter, N.P., Schmidt, B.E., Lawson, J., Shepherd, J.E.: SDToolbox: Numerical Solution Methods for Shock and Detonation Jump Conditions. GALCIT Report FM2018.001, California Institute of Technology, Pasadena, CA (2023)

37. Goodwin, D.G., Moffat, H.K., Schoegl, I., Speth, R.L., Weber, B.W.: Cantera: An Object-Oriented Software Toolkit for Chemical Kinetics, Thermodynamics, and Transport Processes, Version 3.0.0 (2023). https://www.cantera.org/

38. Smith, G.P., Tao, Y., Wang, H.: Foundational Fuel Chemistry Model Version 1.0 (FFCM-1) (2016). https://web.stanford.edu/group/haiwanglab/FFCM1/pages/FFCM1.html

39. Hastie, J.W.: Molecular basis of flame inhibition. J. Res. Natl Bureau Stand. Sect. A Phys. Chem. **77**(6), 733–754 (1973). https://doi.org/10.6028/jres.077a.045